Mode-locked laser operation of Indium-modified Yb:$KY(WO_4)_2$ single crystal

Elena Castellano-Hernández,[1] Xiumei Han,[1] Mauricio Rico,[2] Luis Roso,[2] Concepción Cascales,[1] and Carlos Zaldo[1,*]

[1]*Instituto de Ciencia de Materiales de Madrid. Consejo Superior de Investigaciones Científicas. c/ Sor Juana Inés de la Cruz 3. E-28049 Madrid. Spain*

[2]*Centro de Láseres Pulsados (CLPU). Parque Científico. E-37185 Villamayor. Salamanca. Spain*

[*]*cezaldo@icmm.csic.es*

Abstract: We report the first pulsed laser operation of an Indium-modified Yb:$KY(WO_4)_2$ crystal. Indium incorporation enlarges the broadening of the Yb^{3+} optical bands, reduces crystal lattice parameters and increases n_p refractive index. A $KY_{0.8}In_{0.07}Yb_{0.13}(WO_4)_2$ crystal pumped at 981 nm with a Ti-sapphire laser in a SESAM modulated resonator produces at 300 K self-starting and stable mode-locking. The shortest laser pulses achieved were centred at λ = 1041.1 nm, have a duration of 96 fs with average power of 134 mW and repetition rate of 103.5 MHz (1.3 nJ/pulse).

OCIS codes: (140.3615) Lasers, ytterbium; (140.4050) Mode-locked lasers; (160.3380) Laser materials.

References and links

1. M. Dubinskii, V. Fromzel, N. Ter-Gabrielyan, M. D. Serrano, D. E. Lahera, C. Cascales, and C. Zaldo, "Spectroscopic characterization and laser performance of resonantly diode-pumped Er^{3+}-doped disordered $NaY(WO_4)_2$," Opt. Lett. **36**(16), 3263–3265 (2011).
2. V. Petrov, M. C. Pujol, X. Mateos, O. Silvestre, S. Rivier, M. Aguiló, R. M. Solé, J. Liu, U. Griebner, and F. Díaz, "Growth and properties of $KLu(WO_4)_2$, and novel ytterbium and thulium lasers based on this monoclinic crystalline host," Laser Photon. Rev. **1**(2), 179–212 (2007).
3. A. A. Kaminskii, "Laser crystals and ceramics: recent advances," Laser Photon. Rev. **1**(2), 93–177 (2007).
4. P. V. Klevtsov and R. F. Klevtsova, "Polymorphism of the double molybdates and tungstates of mono- and trivalent metals with the composition $M^+R^{3+}(EO_4)_2$," J. Struct. Chem. **18**(3), 339–355 (1977).
5. M. Pollnau, Y. E. Romanyuk, F. Gardillou, C. N. Borca, U. Griebner, S. Rivier, and V. Petrov, "Double tungstate lasers: From bulk toward on-chip integrated waveguide devices," IEEE J. Sel. Top. Quantum Electron. **13**(3), 661–671 (2007).
6. E. Castellano-Hernández, X. Han, C. Cascales, and C. Zaldo, "Indium-modified Yb:$KY(WO_4)_2$ crystals. Growth, spectroscopy and laser operation," in *Advanced Solid-State Lasers* (Optical Society of America, 2013) paper AWA.2.
7. A. A. Kaminskii, A. F. Konstantinova, V. P. Orekhova, A. V. Butashin, R. F. Klevtsova, and A. A. Pavlyuk, "Optical and nonlinear laser properties of the χ3-active monoclinic α-$KY(WO_4)_2$ crystals," Crystallogr. Rep. **46**(4), 665–672 (2001).
8. P. Wasylczyk, P. Wnuk, and C. Radzewicz, "Passively modelocked, diode-pumped Yb:KYW femtosecond oscillator with 1 GHz repetition rate," Opt. Express **17**(7), 5630–5635 (2009).
9. A. G. Selivanov, I. A. Denisov, N. V. Kuleshov, and K. V. Yumashev, "Nonlinear refractive properties of Yb^{3+}-doped $KY(WO_4)_2$ and YVO_4 laser crystals," Appl. Phys. B **83**(1), 61–65 (2006).
10. H. Liu, J. Nees, and G. Mourou, "Diode-pumped Kerr-lens mode-locked Yb:$KY(WO_4)_2$ laser," Opt. Lett. **26**(21), 1723–1725 (2001).
11. A. A. Lagatsky, C. T. A. Brown, and W. Sibbett, "Highly efficient and low threshold diode-pumped Kerr-lens mode-locked Yb:KYW laser," Opt. Express **12**(17), 3928–3933 (2004).
12. S. Rivier, V. Petrov, A. Gross, S. Vernay, V. Wesermann, D. Rytz, and U. Griebner, "Diffusion bonding of monoclinic Yb:$KY(WO_4)_2$/$KY(WO_4)_2$ and its continuous-wave and mode-locked laser performance," Appl. Phys. Express **1**(12), 112601 (2008).
13. A. A. Demidovich, A. N. Kuzmin, G. I. Ryabtsev, M. B. Danailov, W. Strek, and A. N. Titov, "Influence of Yb concentration on Yb:KYW laser properties," J. Alloy. Comp. **300–301**, 238–241 (2000).
14. S. Rivier, V. Petrov, A. Gross, S. Vernay, V. Wesermann, D. Rytz, and U. Griebner, "Segmented grown Yb:$KY(WO_4)_2$/$KY(WO_4)_2$ for use in continuous-wave and mode locked lasers," Opt. Express **15**(24), 16279–16284 (2007).

#233659 - $15.00 USD Received 30 Jan 2015; revised 6 Mar 2015; accepted 9 Mar 2015; published 21 Apr 2015

15. A. Jasik, J. Muszalski, K. Pierściński, M. Bugajski, V. G. Talalaev, and M. Kosmala, "Low-temperature grown near surface semiconductor saturable absorber mirror: Design, growth conditions, characterization, and mode-locked operation," J. Appl. Phys. **106**(5), 053101 (2009).
16. P. Klopp, V. Petrov, U. Griebner, and G. Erbert, "Passively mode-locked Yb:KYWlaser pumped by a tapered diode laser," Opt. Express **10**(2), 108–113 (2002).

1. Introduction

Lanthanide-doped "disordered" single crystals are being increasingly investigated for their use in diode-pumped lasers. In ordered laser crystals, like YAG, the trivalent lanthanide (Ln^{3+}) and other crystal constituents each occupies a unique crystal site, therefore the Ln^{3+} shows spectrally narrow optical absorption (OA) and photoluminescence (PL) transitions. However, in disordered crystals Ln^{3+} ions experiment a spatially variable crystalline environment leading to inhomogeneous broadening of their OA and PL bands. Such broadening is useful to minimize the pump absorption changes associated either to thermal drift of the diode emission or to the narrowing of the OA in cryogenically operated laser [1]. Moreover, large bandwidths are required to generate ultrashort (< 100 fs) laser pulses.

Point defects, Ln^{3+} multisites, random distribution of different cations on the same crystal sites, and isovalent or aliovalent substitutions of the host cations are possible ways to induce crystal disorder. The band broadening induced by disorder is accompanied by a decrease in peak OA and PL cross sections (σ_{ABS} and σ_{EMI}, respectively) which makes difficult to attain significant pump absorption over short distances, an essential feature of diode-pumped optical cavities. Therefore, disordered crystals with large $\sigma_{ABS/EMI}$ are particularly desired.

$KLn(WO_4)_2$ monoclinic crystals (space group *C*2/*c*, Nº 15), with Ln = Y^{3+}, Gd^{3+}, or Lu^{3+} (Ln siting at a unique eight-oxygen coordinated site, 4*e* Wyckoff position, with C_2 local symmetry) are well established laser crystals characterized by very large OA and PL cross sections for the N_m direction of the indicatrix [2]. Laser action of Nd, Yb, Tm or Ho-doped $KLn(WO_4)_2$ crystals has been shown under continuous wave (cw), Q-switched and mode-locked operation regimes [3]. The monoclinic phase is found for Ln = Sm-Lu [4]. Crystal distortion in this host can be achieved by isovalent substitution of Ln^{3+} by other cations with different ionic radii. From this point of view, In^{3+} may have a significant influence because its ionic radius for VIII-coordination, 0.92 Å, is smaller than any other Ln^{3+} or Y^{3+}, namely the smallest one for VIII-coordination corresponds to Lu^{3+}, 0.977 Å. Additionally, Indium incorporation into $KLn(WO_4)_2$ may change the refractive index (n) and structural lattice parameters, helping to tailor the design of waveguided lasers of this crystal class [5].

In this work we show the successful growth of $KY_{1-x-y}In_xYb_y(WO_4)_2$ monoclinic crystals to achieve an adequate compromise between bandwidth and peak cross section. We report their optical and spectroscopic properties and show the generation of ultrashort (< 100 fs) laser pulses by passive mode-locking.

2. Crystal growth and structural analysis

$KY_{1-x-y}In_xYb_y(WO_4)_2$ crystals have been grown by the top seeded solution growth method. Details of the growth procedures have been given previously [6]. Briefly, Indium incorporation into the monoclinic phase is limited to about x = 0.25. For larger In concentration the monoclinic phase coexists with a trigonal (space group $P\bar{3}c1$, Nº 165) one. In order to avoid phase competition we grew $KY_{0.9-y}In_{0.1}Yb_y(WO_4)_2$ crystals with y = 0.002 and 0.1 (10 at% In and 0.2% or 10 at% Yb). The y = 0.1 grown crystal was analyzed by single crystal X-ray diffraction. The monoclinic *C*2/*c* structure of the crystal and the Y, In and Yb incorporation in the 4*e* Wickoff site were confirmed. The crystal lattice parameters obtained are a = 10.625(3) Å, b = 10.334(2) Å, c = 7.5368(16) Å and β = 130.671(8)°, with cell volume 627.6(2) $Å^3$. As expected, these lattice parameters are smaller than those of $KY(WO_4)_2$ crystal, i.e. a = 10.631 Å, b = 10.345 Å, c = 7.555 Å and β = 130.752°, V = 629.43 $Å^3$. The structure refinement yielded the $KY_{0.8}In_{0.07}Yb_{0.13}(WO_4)_2$ crystal formula, i.e. In is

#233659 - $15.00 USD Received 30 Jan 2015; revised 6 Mar 2015; accepted 9 Mar 2015; published 21 Apr 2015

incorporated to the lattice (7 at%) in a lower amount that it was in the growth solution (10 at%), this deficiency is compensated by extra incorporation of Yb (13 at%), that in the solution was only at 10 at%.

3. Optical and spectroscopic characterization

Figure 1(a) shows the 300 K n(λ) dispersion of the $KY_{0.898}In_{0.10}Yb_{0.002}(WO_4)_2$ crystal measured parallel to the 2-fold *b* crystal axis (N_p direction of the indicatrix). The minimum deviation angle method and a crystal prism were used for this purpose. The limited size of the available crystals prevented prism preparation for other directions of the indicatrix. Compared to $KY(WO_4)_2$ crystal [7] n_p increases. Due to the low Yb concentration this change is attributed to the substitution of Y by In. The $n_p(\lambda)$ results are fit to the Sellmeier law:

$$n^2 = A + \frac{B\lambda^2}{\lambda^2 - C^2} - D\lambda^2. \quad (1)$$

A best fit was obtained with A = 2.342, B = 1.5185, C = 193.3 nm, D = 1.306×10^{-8} nm^{-2}. The group velocity dispersion (GVD) of the crystal was calculated as:

$$GVD = \frac{\lambda^3}{2\pi c^2}\left(\frac{d^2 n}{d\lambda^2}\right). \quad (2)$$

GVD results are shown in Fig. 1(a). Although these values do not correspond to the sample and orientation later used for mode-locking, a first estimation of the In effect can be obtained. The GVD of $KY_{0.898}In_{0.10}Yb_{0.002}(WO_4)_2$ crystal at λ = 1041 nm is 151 fs^2/mm, i.e. slightly smaller than that of 10 at% Yb:$KY(WO_4)_2$, 200 fs^2/mm [8].

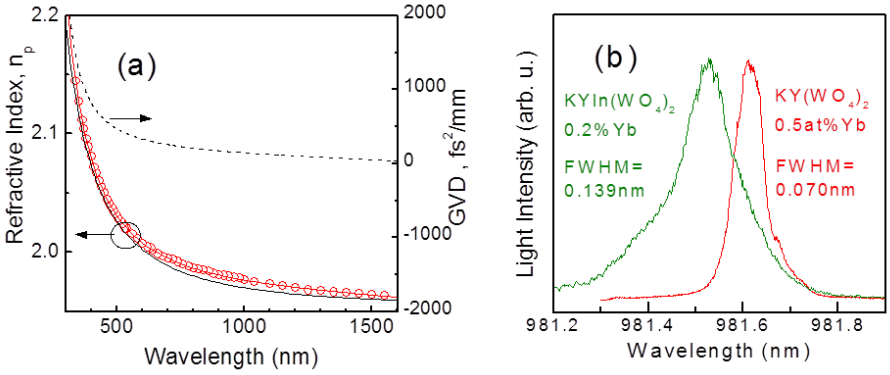

Fig. 1. (a) $KY_{0.898}In_{0.10}Yb_{0.002}(WO_4)_2$ crystal: 300 K n_p refractive index dispersion (open circles), its fit to the Sellmeir law (red continuous line) and group velocity dispersion, GVD (dashed line). To compare, the black continuous line shows n_p for $KY(WO_4)_2$, Ref. 7. (b) Comparison of the $^2F_{7/2}(0)\rightarrow{}^2F_{5/2}(0')$ 6 K excitation PL spectra of Yb^{3+} in $KY_{0.995}Yb_{0.005}(WO_4)_2$ and $KY_{0.898}In_{0.10}$ $Yb_{0.002}(WO_4)_2$ crystals. λ_{EMI} = 1031 nm.

The peak N_m σ_{ABS} = 1.23×10^{-19} cm^2 of Yb^{3+} in $KY_{1-x-y}In_xYb_y(WO_4)_2$ crystals [6], is lower than the corresponding value for Yb:$KY(WO_4)_2$, namely σ_{ABS} = 1.7×10^{-19} cm^2 [10], but still significantly larger than most of Yb-doped laser crystals.

At 300 K the OA of Yb^{3+} is the result of the overlap of transitions from several Stark levels of the ground $^2F_{7/2}$ multiplet. This hampers the identification of the bandwidth of the $^2F_{7/2}(0)\rightarrow{}^2F_{5/2}(0')$ transition and hides the Indium contribution to the inhomogeneous broadening of Yb^{3+}. However, at 6 K the electronic population of the ground $^2F_{7/2}$ multiplet is confined in its lowest energy Stark level, therefore this OA provides such information. Figure 1(b) shows the excitation spectra (formally equivalent to OA) obtained with a Spectra Physics

#233659 - $15.00 USD Received 30 Jan 2015; revised 6 Mar 2015; accepted 9 Mar 2015; published 21 Apr 2015

MOPO system whose emission linewidth is lower than 0.005 nm. While the OA lineshape of 0.5 at% Yb doped $KY(WO_4)_2$ crystal is rather symmetric peaking at 981.61 nm and with a full width at half maximum FWHM = 0.070 nm, the corresponding band observed in the $KY_{0.898}In_{0.10}Yb_{0.002}(WO_4)_2$ crystal shows overlapped side bands, its maximum is shifted to 981.53 nm and the bandwidth increases to FWMH = 0.139 nm. These results evidence the contribution of In to the inhomogeneous broadening the Yb^{3+} transitions.

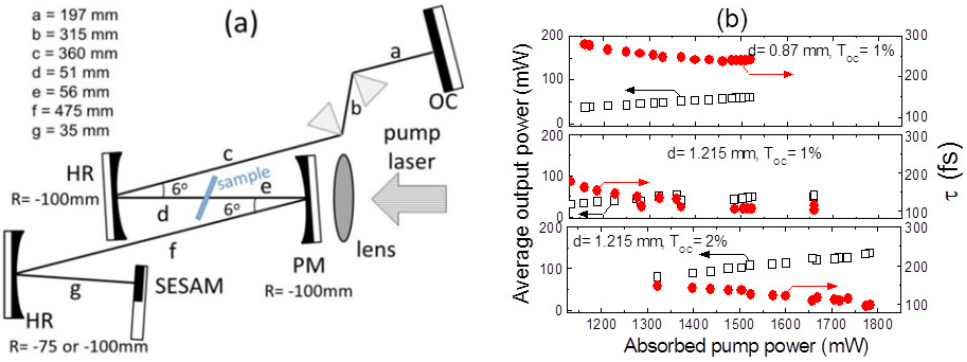

Fig. 2. (a) Astigmatically compensated optical resonator used for mode-locked laser operation. (b) Overview of laser efficiencies (open squares) and pulse duration (τ, full circles) obtained with two sample thickness and two output couplers.

4. Laser characterization

The cw laser operation at 300 K of $KY_{0.8}In_{0.07}Yb_{0.13}(WO_4)_2$ was previously reported [6]. In the present work we test this crystal in the astigmatically compensated z-shaped optical cavity shown in Fig. 2(a). The cavity mode $1/e^2$ diameter at the sample position was 48 μm. The Ti-sapphire pump (λ = 981 nm, horizontally polarized) was focused onto the sample with a f = 62.9 mm lens to a beam waist $1/e^2$ diameter of 50 μm, matching well the cavity mode size. The non-coated sample was passively cooled at 291 K and sets at Brewster angle (with N_m direction also in the horizontal plane) near to the central position between a high reflector (HR, at ≈1000-1050 nm, radius of curvature R_{OC} = −100 mm) and a pumping mirror (PM, R_{OC} = −100 mm), both tilted ≈6°. By using further HRs with different radius, R_{OC} = −100 mm or −75 mm, the intracavity beam was focused onto the semiconductor saturable mirror (SESAM) to a spot with $1/e^2$ diameter of 176 and 124 μm, respectively. A pair of SF10 prisms were used for intracavity GVD compensation and plane output couplers with transmissions T_{OC} = 1 and 2% were tested. Two SESAM mirrors (absorbance 2%, reflectivity >96% in the 1010-1090 nm region, saturation fluence 60 μJ/cm^2, damage threshold 4 mJ/cm^2) purchased from BATOP Optoelectronics were used, their relaxation time was 1ps and 500 fs, respectively. Both provided similar pulse duration, τ, but the latter produced better stability. The output laser beam profile was monitored by a Gentec camera. τ was measured with a APE autocorrelator, while the pulse repetition rate and its frequency distribution were sensed with an Alphalas Si photodetector (risetime <300ps) and recorded in an oscilloscope. The spectral distribution of the laser pulses was monitored with a Wavescan spectrometer and the average output power was measured with a Gentec thermopile.

We tested two samples with thickness d = 0.87 mm (≈80% pump absorption) and d = 1.215 mm (≈100% pump absorption). Figure 2(b) shows an overview of the obtained results. The shortest pulses were obtained with the thickest sample. It seems likely that higher pump absorption of this sample leads to larger intracavity powers and fluence on the SESAM. Hereafter, we will limit the laser result description to the thickest sample.

#233659 - $15.00 USD Received 30 Jan 2015; revised 6 Mar 2015; accepted 9 Mar 2015; published 21 Apr 2015

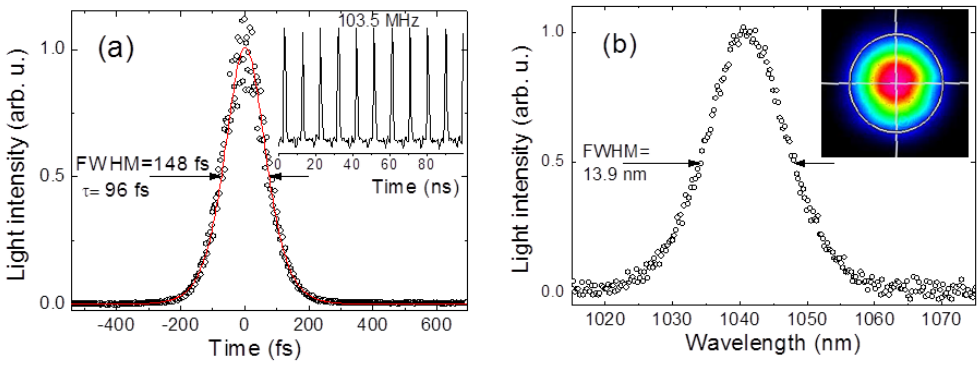

Fig. 3. Characteristics of the mode-locked laser pulses obtained with $KY_{0.8}In_{0.07}Yb_{0.13}(WO_4)_2$ crystal. (a) Autocorrelation trace (open circles) and its fit to a $sech^2$ function (line). The inset shows a mode-locked pulse train. (b) Spectral distribution of the mode-locked pulses. The inset shows the cross section of the beam intensity.

The shortest laser pulses with the $KY_{0.8}In_{0.07}Yb_{0.13}(WO_4)_2$ (d = 1.215 mm) sample were obtained with a tip-to-tip prism distance of 315 mm and a total cavity length of 1490 mm. Mode-locked pulses were observed for absorbed pump powers P_{abs}> 600 mW, but near this threshold the operation was unstable. Stable mode-locking required P_{abs}> 1300 mW. In this stable regime, τ decreases and the average output power P_{out} increases with increasing P_{abs}, see Fig. 2(b). Figure 3 shows the characteristics of a representative laser pulse obtained with a fluence of ≈500 μJ/cm^2 on the SESAM and a T_{OC} = 2%. Figure 3(a) shows that the autocorrelation curve is well fit to a $sech^2$ function, with FWHM = 148 fs, providing τ = 96 fs. Figure 3(b) shows the spectral distribution of these pulses with a maximum at λ = 1041.1 nm and FWHM = 13.9 nm, this implies a time-bandwidth product τ × Δν = 0.370, i.e. still above the Fourier limit, τ × Δν = 0.315. The repetition frequency of these pulses was 103.5 MHz, see Fig. 3(a) inset, and P_{out} = 134 mW, i.e. an average pulse energy of 1.3 nJ. A TEM00 beam quality was observed with an ellipticity of 94.1%, see Fig. 3(b) inset. The laser pulses were slightly tuned (≈2 nm) by varying the GVD compensation.

Table 1 summarizes the most significant results of mode-locked operation obtained with $Yb:KY(WO_4)_2$ crystals. The comparison of the laser performance of our In-modified $Yb:KY(WO_4)_2$ crystal with those previously reported for $Yb:KY(WO_4)_2$ crystal is not straightforward because of the large variety of experimental conditions. Laser characteristics depend strongly on the inversion ratio, i.e. on $^2F_{5/2}$ Yb^{3+} lifetime and temperature. The former decreases with Yb concentration, while the temperature rise increases the population of the $^2F_{7/2}$(n≠ 0) Stark levels reducing the inversion ratio. For the nominal 10 at% Yb concentration used in the present work pulses obtained directly from the oscillator were shorter only by Kerr lens mode-locking when the geometry of the sample allowed N_p polarization [10], since in this case the optical bandwidth is larger than for N_m polarization. Pulse duration of N_m polarized pulses reported by Kerr lens mode-locking of 10 at% $Yb:KY(WO_4)_2$ [11] is in fact slightly longer than that here reported for the In-modified $Yb:KY(WO_4)_2$ crystal. Pulses shorter than those here presented and better laser efficiency were obtained only with 5 at% Yb concentration using diffusion bonded $KY_{0.95}Yb_{0.05}W(WO_4)_2/KY(WO_4)_2$ crystals [12]. This likely corresponds to a better dissipation of the heat generated in the sample, lower reabsorption losses, and to a longer Yb lifetime. In fact, for cw operation it was observed that the laser threshold increases with Yb concentration. For the same absorbed pump power the laser output power decreases only slightly from 5 at% to 10 at% Yb, but much significantly in the 10 at% to 20 at% Yb concentration range [13]. Other works on $Yb:KY(WO_4)_2$ mode-locked lasers [14–16] report longer pulse durations than those here obtained with the In-modified $Yb:KY(WO_4)_2$ crystal.

#233659 - $15.00 USD Received 30 Jan 2015; revised 6 Mar 2015; accepted 9 Mar 2015; published 21 Apr 2015

Table 1. Summary of mode-locking laser results obtained with Yb-doped $KY(WO_4)_2$ crystals. λ_{PUMP} = Pump wavelength. λ_{EMI} = Laser emission wavelength. pol = Polarization. τ = Pulse duration. <E> = Average output power. f = Repetition frequency. $\tau \times \Delta\nu$ = Time bandwidth product. KL = Kerr lens. SESAM = Semiconductor saturable mirror. Ti-sa = Ti-sapphire laser. DL = diode laser. N_p, N_m and N_g refer to the directions of the indicatrix.

Crystal details	Modulation technique	λ_{PUMP} (nm)	λ_{EMI}, pol (nm)	τ (fs)	<E> (mW)	f (MHz)	$\tau \times \Delta\nu$	Ref.
$KY_{0.8}In_{0.07}Yb_{0.13}(WO_4)_2$ N_p-cut	SESAM	Ti-sa, 981	1041, N_m	96	134	103.5	0.370	
$KY_{0.9}Yb_{0.1}(WO_4)_2$	KL	DL, 940	1057, N_p	71	120		0.4	[10]
$KY_{0.9}Yb_{0.1}(WO_4)_2$, N_p-cut	KL	DL, 980.5	1055, N_m	107	126	294	0.32	[11]
$KY_{0.95}Yb_{0.05}(WO_4)_2/KY(WO_4)_2$	InGaAs	Ti-sa, 981	1029, N_m	66	182	93	0.43	[12]
Diffusion bonding, N_p-cut	SAM							
$KY_{0.9}Yb_{0.1}(WO_4)_2/KY(WO_4)_2$	InGaAs	Ti-sa, 981	1029, N_m	99	69	92	0.353	[14]
Segmented growth, N_p-cut	SAM							
$KY_{1-y}Yb_y(WO_4)_2$	InGaAs	DL, 980	1049	101	16	83.7	0.358	[15]
	SAM			110	150		0.372	
$KY_{0.95}Yb_{0.05}(WO_4)_2$	SESAM	TDL, 978	1046	101	100	95	0.34	[16]
			1045	134	150			

5. Summary

In^{3+}, with small ionic radius, is incorporated to the $KY(WO_4)_2$ monoclinic structure up to ≈25 at% with regards to the Y position. $KY_{1-x-y}In_xYb_y(WO_4)_2$ crystals have been grown by the top seeded solution growth method. In incorporation reduces the crystal lattice parameters and enlarges n_p refractive index with regards to the parent $KY(WO_4)_2$ crystal, therefore it may help to design waveguided lasers based on this monoclinic structure. In also increases the bandwidth of the $^2F_{7/2}(0) \rightarrow {}^2F_{5/2}(0')$ Yb^{3+} transition. The $KY_{0.8}In_{0.07}Yb_{0.13}(WO_4)_2$ grown crystal tested in a SESAM modulated z-shaped oscillator produced laser pulses as short as 96 fs at 1041.1 nm with average output power of 134 mW. Further increase of the inhomogeneous broadening of Yb^{3+} bands and the corresponding reduction of the pulse duration are envisaged by increasing the In^{3+} incorporation up to the stability limit of the monoclinic phase.

Acknowledgments

Work supported by the Spanish Ministry of Economy and Competitiveness and by the European Regional Development Fund through MAT2011-29255-C02-01, MAT2014-56607, IPT2011-1121-020000, FIS2013-47741 and Laserlab-III-Ref. 284464 projects. E. C. is supported by the BES-2012-060296 grant.